The Canadian Mineralogist
Vol. 46, pp. 1183-1194 (2008)
DOI: 10.3749/canmin.46.5.1183

KARELIANITE AND VANADIAN PHLOGOPITE FROM THE MERELANI HILLS GEM ZOISITE DEPOSITS, TANZANIA

GASTON GIULIANI[§]

IRD (Institut de Recherche pour le Développement, UR154 LMTG) and CRPG, Nancy-Université, CNRS, BP 20, F–54501 Vandœuvre-lès-Nancy, France

DANIEL OHNENSTETTER[§], FABIEN PALHOL, JULIEN FENEYROL, EMILIE BOUTROY AND HÉLÈNE DE BOISSEZON

CRPG, Nancy-Université, CNRS, BP 20, F–54501 Vandœuvre-lès-Nancy, France

THÉRÈSE LHOMME

UMR G2R, Nancy-Université, BP 239, F–5450 Vandœuvre-lès-Nancy, France

ABSTRACT

The Merelani deposits of gem-quality vanadian zoisite ("tanzanite") in Tanzania occur in Proterozoic vanadium-rich sedimentary series metamorphosed to the amphibolite facies. The gem-bearing assemblage consists of quartz, sulfides, graphite and "tanzanite" occurring in hydrothermal veins deposited in hydrothermally altered graphitic gneisses, marbles and calc-silicates. Two rare vanadian oxide and silicate minerals crystallize on the margins of pyrite and V-bearing pyrrhotite lenses, which are cross-cut by graphite–"tanzanite"-bearing quartz veins. Karelianite has a nearly pure end-member composition in the karelianite–eskolaite solid-solution series, with 93 to 96 wt% V_2O_3. Vanadian phlogopite closely associated with karelianite has high MgO (18.5 to 22.8 wt%), F (1.2 to 2.0 wt%) and TiO_2 (up to 1.3 wt%). The V_2O_3 content varies between 4.2 and 10.9 wt%. The protolith of the host rock that contains the mineralization is a black shale; the hydrothermal graphite has a $\delta^{13}C$ equal to –24.0‰, which indicates a sedimentary source rich in organic matter. During hydrothermal alteration, V and Cr were scavenged by fluids from the graphitic gneisses, and fixed by the oxide and silicates. Textural evidence of dissolution of karelianite indicates that vanadium was remobilized by the hydrothermal fluid during the formation of late-stage vanadian zoisite ("tanzanite"), found in veinlets that cross-cut both sulfides and vanadium-bearing minerals.

Keywords: karelianite, vanadian phlogopite, tanzanite, graphitic gneiss, Merelani, Mozambique Belt, Tanzania.

SOMMAIRE

Les gisements de gemmes de zoïsite vanadifère ("tanzanite") de Merelani, en Tanzanie, sont contenus dans des séries protérozoïques d'origine sédimentaire métamorphisées dans le faciès amphibolite. La zone minéralisée est formée par des veines de quartz à sulfures, graphite et "tanzanite" qui recoupent les gneiss graphiteux, les marbres et les roches calco-silicatées altérées hydrothermalement. La karélianite et une phlogopite vanadifère sont formées en bordure de lentilles de pyrite et de pyrrhotite vanadifère, et recoupées par des veines à quartz–graphite et "tanzanite". La karélianite, avec une composition en V_2O_3 comprise entre 93 à 96% (poids), est donc proche du pôle vanadifère de la solution solide karélianite–eskolaïte. La phlogopite vanadifère est associée intimement à la karélianite; la teneur en MgO est élevée (18.5 à 22.8%, poids) tout comme celle en F (1.2 à 2.0%, poids) et TiO_2 (jusqu'à 1.3%, poids). La teneur en V_2O_3 varie entre 4.2 et 10.9 % (poids). Le protolithe de la roche hôte qui contient la minéralisation est un schiste noir; la valeur du $\delta^{13}C$ du graphite hydrothermal, –24.0‰, indique pour le carbone une source organique et sédimentaire. Au cours de l'altération hydrothermale, le V et Cr contenus dans les gneiss graphiteux ont été mobilisés par les fluides et fixés par l'oxyde et les silicates vanadifères. Des évidences de dissolution de la karélianite indiquent que le vanadium a été remobilisé par le fluide hydrothermal au cours de la formation des veinules et des veines à "tanzanite" qui recoupent les lentilles de sulfures et les minéraux à vanadium.

Mots-clés: karélianite, phlogopite vanadifère, tanzanite, gneiss graphiteux, Merelani, ceinture Mozambicaine, Tanzanie.

§ *E-mail addresses*: giuliani@crpg.cnrs-nancy.fr, dohnen@crpg.cnrs-nancy.fr

Introduction

The Merelani Hills deposits of vanadium-bearing zoisite ("tanzanite"), in Tanzania, occur in V-rich graphitic schists and are characterized by several vanadium-bearing minerals (Walton & Marshall 2007). The association of "tanzanite", a vanadium-rich member of the zoisite subgroup (Hurlbut 1969), with "tsavorite", a vanadium-rich member of the garnet group (Bridges 1982) has yielded two new gem minerals introduced on the gem market within the last 25 years. No systematic mineralogical and chemical studies of the mineralized rocks are yet available. In samples of the Merelani ore, karelianite and vanadium-rich phlogopite were identified in graphite-bearing quartz veinlets formed along the edge of pyrrhotite–pyrite lenses. In this study, we present the first results concerning the mineral composition and textural features of these vanadium-rich oxide and micas and their significance. The presence of vanadium-bearing minerals in the carbonaceous host-rock formed during the metamorphic and hydrothermal stages of the deposit is compared with other vanadium-enriched lithologies and ore deposits worldwide.

Background Information

The rare vanadium oxide mineral *karelianite* was first described in the Outokumpu district of Finnish Karelia, in a large volcanogenic Cyprus-type Cu–Co–Zn deposits (Long *et al*. 1963, von Knorring *et al*. 1986, Treloar 1987). Other occurrences are from the metamorphosed Pb–Zn–(Ag) sedimentary-exhalative Rampura Agucha deposit in Rajasthan, India (Höller & Stumpfl 1995), and the primary U–V ores from the Mounana uranium mine in Gabon (Gauthier-Lafaye & Weber 2003). It is also found in vanadiferous anthraxolite bitumen from Guangxi in China (Liu & Lin 1984), as well as in the Hemlo mesothermal gold deposit in Canada (Harris 1989). There is a continuous solid-solution series between the two end-members eskolaite (Cr_2O_3) and karelianite (V_2O_3). Members of that solid-solution series in association with schreyerite, olkhonskite and rutile are also reported in the graphite-bearing sillimanite quartzite schists of the Olkhon series, Baikal region, Russia, by Koneva (2002). Karelianite is also found associated with dessauite in alpine hydrothermal veins developed in a hematite–barite ore within dolomite in the Buca della Vena mine in northern Tuscany (Orlandi *et al*. 1997). Vanadian minerals are associated worldwide with remobilization of V and Cr from two different sources: either mafic–ultramafic rocks (Treloar 1987, Pan & Fleet 1992), or black shales interbedded with limestones and sandstones (Orlandi *et al*. 1997, Koneva 2002, Gauthier-Lafaye & Weber 2003).

Geological Setting

The Merelani area lies at 65 km southeast of the town of Arusha in northeastern Tanzania. It belongs to the eastern granulitic complex of the Neoproterozoic Mozambique belt, which underwent a peak of granulite metamorphism at *ca*. 640 Ma (Muhongo *et al*. 2001). The "tanzanite" deposits are located in the western limb of a major recumbent fold structure, the Lelatema antiform (Malisa 1987). "Tanzanite" is commonly found either in cavities at the hinge of folds in quartz veins (Malisa & Muhongo 1990) or interbedded in hydrothermally altered kyanite – sillimanite – biotite – graphite gneisses, marbles and calc-silicates (Muhongo *et al*. 1999). "Tanzanite", Cr-bearing tourmaline and Cr-bearing diopside are concentrated in quartz veins with graphite, pyrite, pyrrhotite and chalcopyrite. High-temperature hydrothermal fluids circulated along fold hinges at temperature between 390 and 450°C and pressure around 3 kbar (Malisa 1998, Muhongo *et al*. 1999).

Naeser & Saul (1974) suggested that "tanzanite" is related to pegmatite, whereas Malisa & Muhongo (1990) proposed that the deposit is formed during hydrothermal circulation of fluids in extensional structures related to the Pan-African orogeny.

The Tanzanian government divided the "tanzanite" mining area into four claims, A to D respectively, in 1991. The C claim is exploited by the company "Tanzanite One"; the other claims are operated by local miners as open pits and underground workings to a depth of 100 m (Zancanella 2006). The exact production of "tanzanite" is still unknown; however, the African Gem Resources company produced 812,526 carats of "tanzanite" between January to September 2003 (Walton & Marshall 2007). For the finest stones of less than 50 carats, prices can reach $1,000 per carat. The largest crystal found in claim D weighs 3368 grams (Zancanella 2006).

Samples and Analytical Techniques

Hand specimens containing karelianite and vanadian phlogopite were collected in claim B. Polished sections were examined under back-scattered electron (BSE) imaging with a Hitachi S–4800 scanning electron microscope (SEM) at the Université Henri-Poincaré, Vandœuvre-lès-Nancy. The electron-probe micro-analyses (EPMA) were obtained on a Cameca SX100. We employed the following operating conditions for the analysis of vanadium oxides: accelerating voltage 15 kV, beam current 10 nA, raster length 0.03 μm, collection times of 15 s for iron and manganese, 30 s for vanadium, and 60 s for chromium, 60 s for titanium,

45 s for magnesium and 30 s for zinc. The samples were analyzed for iron, manganese and vanadium using the *K*α peaks of Fe, Mn and V on a LIF crystal, respectively. Chromium was quantified using the *K*β peak on a PET crystal. Operating conditions for the analysis of vanadium silicates were: accelerating voltage 15 kV, beam current 10 nA, raster length 2 μm, collection times of 10, 20 and 30 s, respectively for major, trace and halogen elements. For the sulfides, the analytical conditions were made with an accelerating voltage of 30 kV, 60 nA, and a counting time of 30 s for Co, Ni and As, and 10 s for Fe and S. We calibrated Fe and S with pyrite, As with arsenopyrite, and Co, Ni, Cr and V with metals.

We used natural and synthetic standards and the PAP program (Pouchou & Pichoir 1991) for data reduction. Compositions expressed in terms of atoms per formula unit (*apfu*) were calculated on the basis of three atoms of oxygen for karelianite and 24 (O, OH, F, Cl) atoms for vanadian phlogopite. We calculated Fe, Mn, Zn, Mg as divalent ions, whereas V, Cr and Al were calculated as trivalent ions. The Raman spectra of karelianite, presented for the first time, and vanadian phlogopite were measured using a Horyba–Jobin Yvon Raman microspectrometer at the Université Henri-Poincaré, UMRG2R, Vandœuvre-lès-Nancy. The microspectrometer is equipped with an edge filter, a holographic grating with 1800 grooves per millimeter, with a liquid-nitrogen-cooled CCD detector. The laser was focused on the sample using a ×80 objective; the excitation radiation was the 514.5 nm line of an Ar^+ green laser (2020 Spectra-physics) that delivered 1 mW at the sample surface. Digital versions of the spectra shown in Figures 5 (karelianite) and 7 (vanadian phlogopite) are available from the Depository of Unpublished Data, MAC website [document Karelianite CM46_1183].

Graphite was prepared for carbon isotope measurements by separating 1 to 2 mg of crystals from the quartz veins and subsequent combustion with excess CuO and Cu_2O at 900°C over three hours. Carbon dioxide was extracted *in vacuo* by heating to 1,500°C using a methane–oxygen torch. The CO_2 was analyzed by mass spectrometry on a VG 602D mass spectrometer at the CRPG–CNRS, with a reproducibility of ±0.1‰.

Mineralogy

Oxide minerals and micas enriched in V and Cr are associated with quartz–graphite-bearing veinlets cross-cutting sulfide lenses (Fig. 1A). Pyrite I and pyrrhotite are coeval, but the pyrrhotite is highly fractured. The grains of karelianite occur at the interface of pyrrhotite, graphite, quartz (Fig. 1B) and vanadian phlogopite (Fig. 2). Karelianite is the first mineral that filled the brecciated pyrrhotite (Figs. 1B, C, 2). Graphite crystals generally cross-cut karelianite (Fig. 1C). The grain boundary of karelianite is mostly irregular and wavy, showing evidence of corrosion and dissolution during the formation of graphite in the quartz veins. Vanadian phlogopite is rare and is closely associated with karelianite (Fig. 2). The vanadian minerals are roughly coeval; although vanadian phlogopite cross-cuts karelianite, locally, they form intergrowths (Fig. 2). Graphite occurs as flakes in fracture fillings with quartz and yellowish to greenish vanadian zoisite and pyrite II. The size of the flakes, which are mostly concentrated along the border of the quartz veins, ranges from 100 μm to 1 cm (Fig. 1B).

"Tanzanite" occurs either as euhedral crystals mm to cm across in the quartz vein or in pyrite II in microfracture fillings of some five to tens of μm that cross-cut the sulfides and the V–Cr mineral assemblages (Fig. 1F). A late retrograde episode of alteration affected the entire assemblage; the contact zones between pyrrhotite and karelianite are outlined by retrograde V–Fe-enriched secondary silicate phases (Figs. 1D, E).

Karelianite

Grains of karelianite are found at the contact with pyrrhotite as a discontinuous rim up to 700 μm wide or as an infilling phase in corroded zones of the pyrrhotite (Fig. 1B). The crystals are free of inclusions but are in some cases partly intergrown with vanadian phlogopite (Fig. 2). Its polishing hardness is greater than that of coexisting sulfides, and its color in reflected light is brownish.

X-ray scanning images show that the karelianite is homogeneous in composition, with a uniform distribution of Cr and V (Fig. 3). Electron-probe micro-analyses performed on several grains show no significant compositional variations (Table 1). The V_2O_3 content ranges from 94 to 96 wt%, and the Cr_2O_3 content from 3.2 to 4.2 wt%. The FeO and TiO_2 contents range from 0.17 to 0.66 wt% and from 0.1 to 0.16 wt%, respectively. The Al_2O_3 content is up to 0.15 wt%, and the MgO content, up to 0.1 wt%. In most cases, MnO and ZnO are below the detection limit. Compositions are very close to the karelianite end-member (Fig. 4) of the solid solution. The Raman lines of karelianite are defined at 219, 354 and 506 cm^{-1} (Fig. 5).

Vanadian phlogopite

Vanadian phlogopite, rarely encountered (Pan & Fleet 1992), is now reported in the Merelani deposits. It shows considerable compositional variations within each grain (Table 2). The Mg contents are high, varying between 18.5 and 22.8 wt% MgO, and consequently Fe is low (0.01 < FeO < 0.44 wt%). The amounts of F and Ti also are high, and range between 1.22 and 2.0 wt%, and 0.38 to 1.29 wt% respectively. Vanadium in the phlogopite varies widely between 4.2 and 10.9 wt% V_2O_3, and chromium is between 0.2 to 1.13 wt% Cr_2O_3 (Table 2). Manganese reaches up to 0.4 wt% MnO, and barium is up to 0.24 wt% BaO. Usually, nickel, calcium

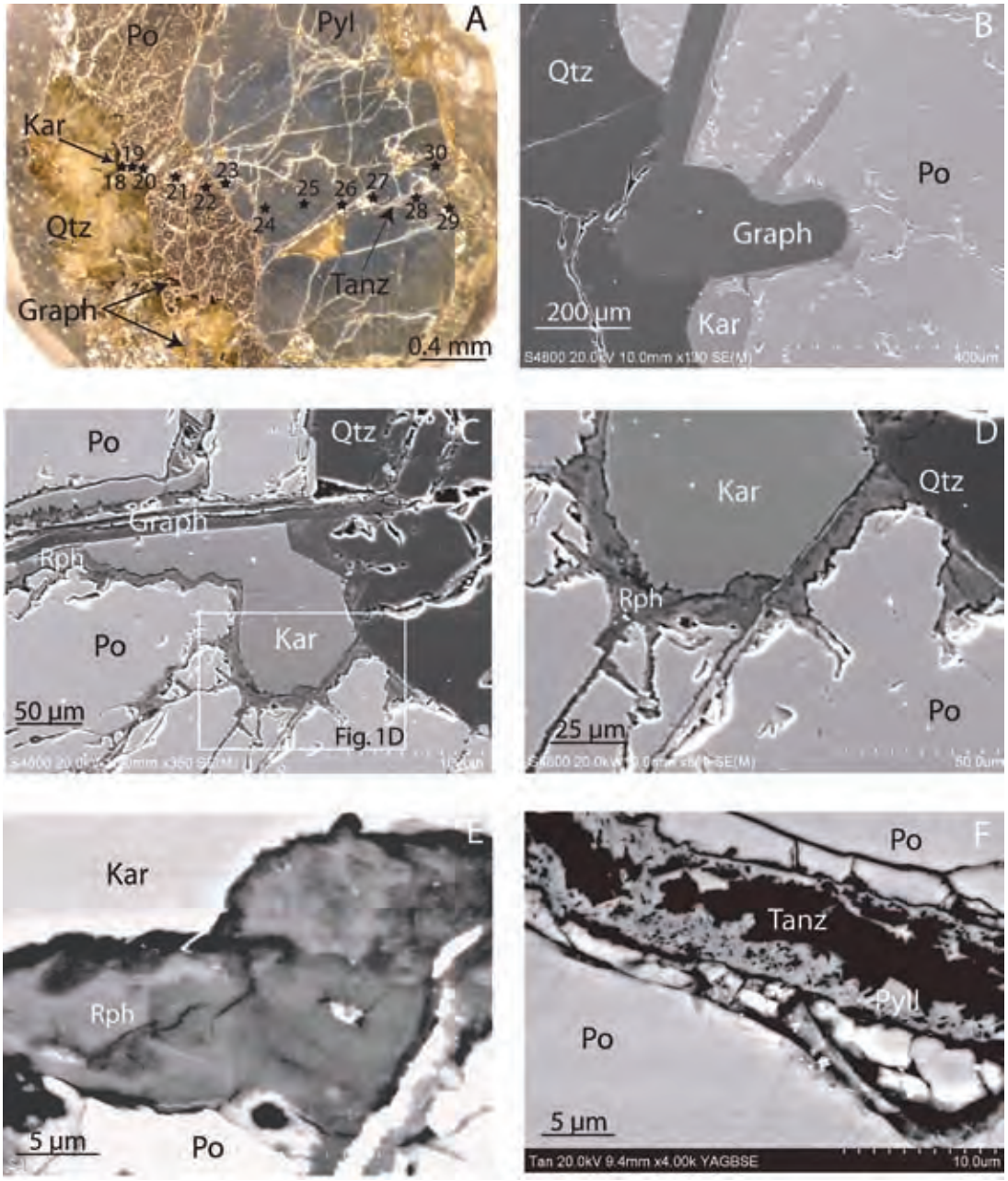

FIG. 1. Photomicrograph (A) and back-scattered electron images (B to F) of the assemblages of vanadium-bearing minerals. A) Pyrrhotite – pyrite lens cross-cut by a graphite-bearing quartz vein. Karelianite is observed at the quartz–graphite contact with pyrrhotite. The sulfides are cross-cut by microveinlets infilled with "tanzanite". The points 18 to 30 represent the location of the EPMA analyses. B) Subhedral grains of karelianite at the interface between pyrrhotite and graphite. C) Graphite-bearing quartz vein cross-cutting karelianite and pyrrhotite. The contact between karelianite and pyrrhotite is emphasized by retrograde minerals. D) Detail of C showing the aspect of the retrograde phases developed at the expense of karelianite and pyrrhotite. E) The retrograde mixtures are composed of micrometric V–Fe silicates formed by the destabilization of karelianite and pyrrhotite, and by elements carried by the fluid during retrograde metamorphic stages. F) Microveinlet of "tanzanite" and pyrite (PyII) cross-cuts pyrrhotite. Symbols: Po: pyrrhotite, Py I, II: pyrite I, II, Graph: graphite, Qtz: quartz, Kar: karelianite, Tanz: "tanzanite", Rph: retrograde phases.

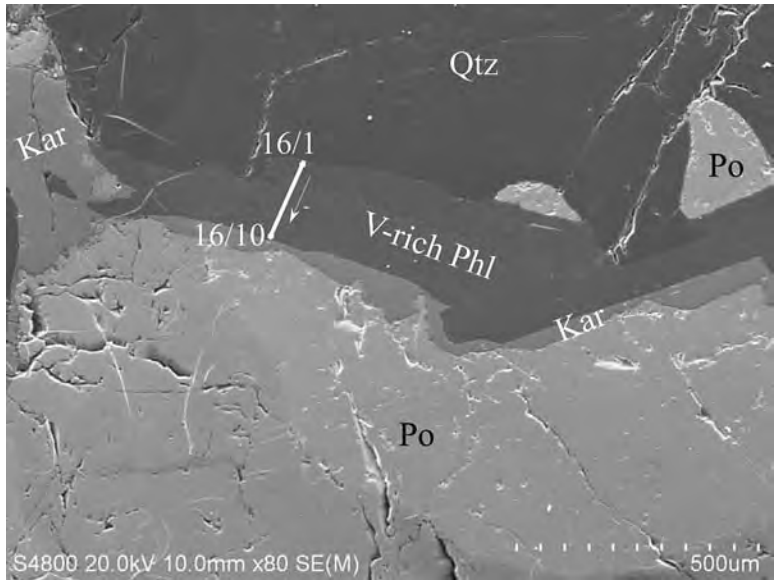

FIG. 2. Association of karelianite and vanadian phlogopite at the interface between pyrrhotite and a quartz (Qtz) vein. The pyrrhotite (Po) has been fractured, and karelianite (Kar) forms a discontinuous rim associated with flakes of vanadian phlogopite. The points 16/1 to 16/10 represent the location of EPMA analyses in the P16 scan. Symbols: Po: pyrrhotite, Qtz: quartz, Kar: karelianite, V-rich Phl: vanadian phlogopite.

TABLE 1. CHEMICAL COMPOSITION OF KARELIANITE FROM THE MERELANI HILLS "TANZANITE" DEPOSITS

Analyses	K1	K2	K3	K4	K5	K6	K7	K8	K9	K10	K11	K12
V_2O_3 wt%	95.99	94.54	95.42	95.55	94.65	94.58	94.82	94.35	94.46	95.68	94.52	95.87
Cr_2O_3	3.44	4.08	3.24	3.57	4.22	3.99	3.81	3.34	3.74	3.42	3.49	3.26
FeO	0.27	0.17	0.42	0.49	0.66	0.41	0.55	0.26	0.18	0.43	0.27	0.26
MnO	0.00	0.00	0.00	0.00	0.00	0.00	0.00	0.00	0.06	0.00	0.00	0.00
TiO_2	0.11	0.11	0.16	0.11	0.10	0.11	0.11	0.10	0.13	0.14	0.03	0.13
Al_2O_3	0.13	0.12	0.09	0.11	0.11	0.12	0.09	0.15	0.12	0.13	0.13	0.09
MgO	0.03	0.10	0.05	0.06	0.02	0.01	0.08	0.06	0.02	0.05	0.06	0.06
Total	99.97	99.12	99.38	99.89	99.76	99.22	99.46	98.26	98.71	99.85	98.50	99.67
Al *apfu*	0.004	0.004	0.003	0.003	0.003	0.004	0.003	0.004	0.004	0.004	0.004	0.003
Cr	0.068	0.081	0.064	0.070	0.083	0.079	0.076	0.067	0.075	0.068	0.070	0.064
Fe^{3+}	0.006	0.004	0.009	0.010	0.014	0.009	0.012	0.006	0.004	0.009	0.006	0.005
Mn^{3+}	0.000	0.000	0.000	0.000	0.000	0.000	0.000	0.000	0.001	0.000	0.000	0.000
V^{3+}	1.919	1.906	1.919	1.912	1.897	1.906	1.906	1.919	1.913	1.915	1.918	1.923
Ti	0.002	0.002	0.003	0.002	0.002	0.002	0.002	0.002	0.002	0.003	0.001	0.002
Mg	0.001	0.004	0.002	0.002	0.001	0.000	0.003	0.002	0.001	0.002	0.002	0.002
Total	2.000	2.001	2.000	2.000	2.000	1.999	2.000	2.000	1.999	2.000	2.001	2.000
Hem mol.%	0.00	0.00	0.00	0.01	0.01	0.00	0.01	0.00	0.00	0.00	0.00	0.00
Kar	0.96	0.96	0.96	0.96	0.95	0.96	0.96	0.96	0.96	0.96	0.96	0.96
Esk	0.04	0.04	0.04	0.04	0.04	0.04	0.03	0.04	0.04	0.04	0.04	0.04

Symbols: Hem: hematite, Kar: karelianite, Esk: eskolaite.

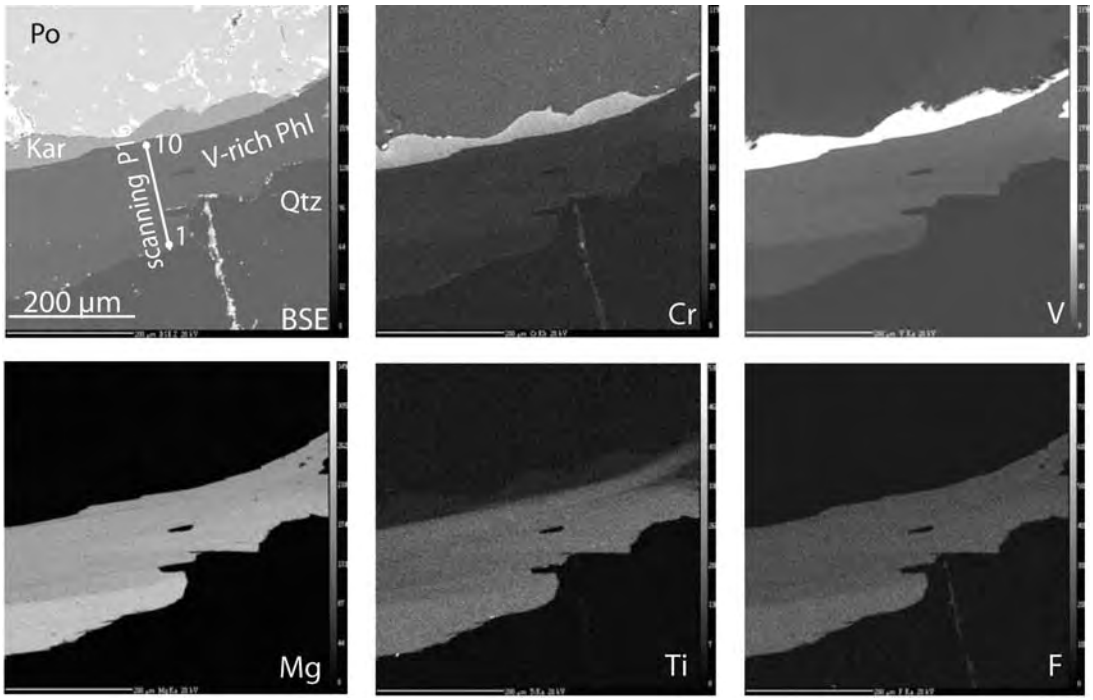

FIG. 3. Back-scattered image (BSE) of the associated karelianite (Kar) and vanadian phlogopite (V-rich Phl) with the different X-ray scanning images taken for the elements: Cr ($K\alpha$), V ($K\alpha$), Mg ($K\alpha$), Ti ($K\alpha$) and F ($K\alpha$). Symbols: Po: pyrrhotite, Qtz: quartz, Kar: karelianite, V-rich Phl: vanadian phlogopite.

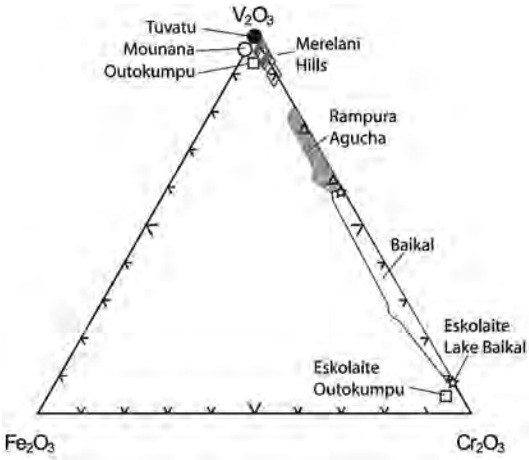

FIG. 4. The chemical composition of karelianite from Merelani Hills, shown in terms of a Cr_2O_3–V_2O_3–Fe_2O_3 diagram. Other chemical compositions reported are from Lake Baikal (Koneva 2002), Outokumpu (Long *et al*. 1963), Tuvatu (Spry & Scherbarth 2006), Mounana (Geffroy *et al*. 1964) and the Rampura Agucha deposit (Höller & Stumpfl 1995).

and chloride contents are below the detection limit. The variation in composition of the vanadium-rich phlogopite is shown by the X-ray scanning images of a single lamella of vanadian phlogopite (Fig. 3). Comparison with the back-scattered image with the X-ray mapping indicates that magnesium is associated with fluorine and titanium. A scanning profile was done along section P16 from points 1 to 10 (Fig. 6, Table 2). The Mg content correlates positively with the F content ($y = 0.1821x - 2.2226$ [$R^2 = 0.94$]). There is a significant replacement of magnesium by vanadium (Fig. 6), producing a high proportion of vacancies at the octahedral positions in the structure (up to 0.6 *apfu*). Consequently, vanadium also correlates with fluorine ($R^2 = -0.87$). Chromium shows a positive correlation with vanadium ($R^2 = 0.71$), as both elements substitute for Mg.

Vanadian phlogopite is defined by its Raman lines at 195, 682 and 1032 cm^{-1} (Fig. 7). The variations in vanadium content, which correlate with fluorine ($R^2 = -0.79$), have no influence on the position of the respective Raman peaks.

TABLE 2. CHEMICAL COMPOSITION OF VANADIAN PHLOGOPITE FROM THE MERELANI HILLS "TANZANITE" DEPOSITS

Anal.	P12	P13	P14	P15	P16/1	P16/2	P16/3	P16/4	P16/5	P16/6	P16/7	P16/8	P16/9	P16/10	P17	P18	P19	P20
SiO_2	39.80	40.05	39.70	39.53	39.53	40.20	40.00	40.70	39.70	39.40	39.25	39.20	39.50	38.78	40.61	41.46	40.50	41.32
TiO_2	1.20	1.25	1.04	1.11	1.21	1.20	1.13	1.06	1.07	1.13	1.07	1.13	1.08	0.38	1.04	1.04	1.29	1.17
Al_2O_3	14.86	14.91	14.78	14.65	14.82	14.72	14.93	15.02	14.65	14.83	14.66	14.66	14.49	14.85	14.27	14.40	14.50	14.45
Cr_2O_3	0.28	0.20	0.45	0.61	0.31	0.34	0.58	0.59	0.50	0.43	0.60	0.65	0.59	1.13	0.69	0.81	0.42	0.74
V_2O_3	4.53	4.63	8.61	9.07	4.77	4.21	6.68	7.28	8.54	7.30	7.87	8.84	9.23	10.88	8.43	7.15	4.49	8.97
FeO	0.22	0.16	0.43	0.20	0.01	0.20	0.19	0.44	0.09	0.19	0.30	0.17	0.26	0.13	0.21	0.21	0.12	0.17
MnO	0.13	0.22	0.25	0.05	0.00	0.10	0.14	0.39	0.02	0.12	0.09	0.14	0.11	0.23	0.13	0.20	0.09	0.11
MgO	22.82	22.69	19.65	19.58	23.26	22.83	20.85	19.52	19.81	20.69	20.59	20.11	19.51	18.50	19.16	19.28	22.39	18.73
CaO	0.00	0.00	0.00	0.70	0.07	0.00	0.00	0.00	0.07	0.00	0.00	0.00	0.00	0.00	0.00	0.00	0.00	0.00
BaO	0.12	0.11	0.10	0.17	0.00	0.11	0.13	0.12	0.11	0.11	0.12	0.13	0.11	0.11	0.13	0.00	0.17	0.00
Na_2O	0.04	0.09	0.00	0.01	0.04	0.03	0.04	0.01	0.05	0.04	0.03	0.00	0.05	0.02	0.04	0.02	0.04	0.04
K_2O	10.23	10.13	9.86	9.81	9.95	10.10	9.92	9.29	9.75	10.08	9.99	9.84	9.93	9.75	9.94	9.83	9.74	9.94
NiO	0.07	0.00	0.04	0.02	0.06	0.07	0.00	0.15	0.00	0.05	0.00	0.01	0.01	0.00	0.00	0.00	0.00	0.02
F	1.78	1.85	1.33	1.48	2.00	1.96	1.62	1.24	1.36	1.64	1.42	1.41	1.35	1.22	1.48	1.60	2.17	1.48
H_2O*	3.36	3.34	3.57	3.52	3.26	3.28	3.44	3.63	3.55	3.41	3.51	3.53	3.55	3.59	3.50	3.46	3.18	3.55
–O=F	-0.75	-0.78	-0.56	-0.62	-0.84	-0.83	-0.68	-0.52	-0.57	-0.69	-0.60	-0.59	-0.57	-0.51	-0.62	-0.67	-0.91	-0.62
Total	98.70	98.85	99.25	99.88	98.45	98.53	98.97	98.92	98.69	98.73	98.91	99.22	99.20	99.06	99.01	98.79	98.18	100.07
Si	5.670	5.689	5.664	5.619	5.633	5.722	5.692	5.780	5.679	5.641	5.619	5.600	5.648	5.577	5.792	5.889	5.773	5.821
^{IV}Al	2.330	2.311	2.336	2.381	2.367	2.278	2.308	2.220	2.321	2.359	2.381	2.400	2.352	2.423	2.208	2.111	2.227	2.179
^{VI}Al	0.165	0.185	0.149	0.074	0.122	0.192	0.196	0.294	0.149	0.143	0.093	0.069	0.089	0.094	0.191	0.300	0.209	0.220
Ti	0.129	0.134	0.112	0.119	0.130	0.128	0.121	0.113	0.115	0.122	0.115	0.121	0.116	0.041	0.112	0.111	0.138	0.124
Cr	0.032	0.022	0.051	0.069	0.035	0.038	0.065	0.066	0.057	0.049	0.068	0.073	0.067	0.128	0.078	0.091	0.047	0.082
V	0.517	0.527	0.985	1.034	0.545	0.481	0.762	0.829	0.980	0.838	0.903	1.013	1.058	1.255	0.964	0.814	0.513	1.013
Fe^{2+}	0.026	0.019	0.051	0.024	0.001	0.024	0.023	0.052	0.011	0.023	0.036	0.020	0.031	0.016	0.025	0.025	0.014	0.020
Mn	0.016	0.026	0.030	0.006	0.000	0.012	0.017	0.047	0.002	0.015	0.011	0.017	0.013	0.028	0.016	0.024	0.011	0.013
Mg	4.846	4.805	4.179	4.149	4.942	4.845	4.423	4.133	4.225	4.416	4.394	4.283	4.158	3.966	4.074	4.083	4.758	3.934
Ni	0.008	0.000	0.005	0.002	0.007	0.008	0.000	0.017	0.000	0.006	0.000	0.001	0.001	0.000	0.000	0.000	0.000	0.002
ΣOct	5.738	5.718	5.561	5.476	5.782	5.728	5.608	5.552	5.539	5.611	5.620	5.597	5.534	5.528	5.459	5.448	5.690	5.409
Ca	0.000	0.000	0.000	0.107	0.011	0.000	0.000	0.000	0.011	0.000	0.000	0.000	0.000	0.000	0.000	0.000	0.000	0.000
Ba	0.007	0.006	0.006	0.009	0.000	0.006	0.007	0.007	0.006	0.006	0.007	0.007	0.006	0.006	0.007	0.000	0.009	0.000
Na	0.011	0.025	0.000	0.003	0.011	0.008	0.011	0.003	0.014	0.011	0.008	0.000	0.014	0.006	0.011	0.006	0.011	0.011
K	1.859	1.836	1.795	1.779	1.809	1.834	1.801	1.683	1.779	1.841	1.825	1.793	1.811	1.789	1.809	1.781	1.771	1.786
ΣInt	1.877	1.867	1.800	1.898	1.831	1.849	1.819	1.693	1.810	1.858	1.840	1.801	1.831	1.801	1.827	1.787	1.792	1.797
F	0.802	0.831	0.600	0.665	0.901	0.882	0.729	0.557	0.615	0.743	0.643	0.637	0.610	0.555	0.668	0.719	0.978	0.659
OH	3.198	3.169	3.400	3.335	3.099	3.118	3.271	3.443	3.385	3.257	3.357	3.363	3.390	3.445	3.332	3.281	3.022	3.341
Total	19.615	19.585	19.362	19.374	19.612	19.576	19.427	19.245	19.349	19.469	19.460	19.398	19.366	19.329	19.286	19.235	19.482	19.206

Compositions are first listed in terms of wt%, then are converted to atoms per formula unit (*apfu*) on the basis of 24 (O, OH, F, Cl). * calculated amount of H_2O.

Graphite

Three crystals of graphite in "tanzanite"-bearing quartz veins (samples from claims B and D) gave $\delta^{13}C$ values (relative to the Pee Dee Belemnite) of –23.3, –23.5, and –25.2‰.

Sulfides

Pyrrhotite contains rare inclusions of chalcopyrite, and pyrite I is free of inclusions. Both minerals are cross-cut by microveinlets of "tanzanite"–pyrite II. Back-scattered electron images show no chemical zoning in the sulfides. Pyrrhotite shows variable concentrations of V and Ni without any significant Co and As (Table 3). Vanadium contents vary between 5,800 and 18,900 ppm. A clear inverse correlation exists between vanadium and iron ($R^2 = –0.99$). The chromium content reaches 1300 ppm, with the highest concentrations of Cr correlated with the highest V content (Table 3). The Ni content is quite uniform and between 9,400 and 11,170 ppm, correlating poorly with iron or sulfur ($R^2 = 0.61$).

Nickel contents in pyrite I attains up to 1700 ppm. The cobalt content varies between 200 and 1000 ppm, and that of As, up to 1000 ppm (Table 3).

TABLE 3. CHEMICAL COMPOSITION OF PYRRHOTITE AND PYRITE FROM THE MERELANI HILLS "TANZANITE" DEPOSITS

	Pyrrhotite					Pyrite							
Analyses	Po 18	Po 19	Po 20	Po 21	Po 22	Py 23	Py 24	Py 25	PY 26	Py 27	Py 28	Py 29	Py 30
V wt%	1.48	0.58	1.27	1.89	0.44	0.06	0.00	0.00	0.00	0.00	0.00	0.00	0.00
Cr	0.00	0.05	0.13	0.00	0.00	0.00	0.00	0.00	0.00	0.00	0.00	0.00	0.00
Fe	57.89	59.38	58.32	58.18	59.69	47.19	47.60	46.78	46.67	46.65	46.33	46.49	46.28
As	0.00	0.05	0.09	0.07	0.08	0.01	0.07	0.04	0.05	0.03	0.10	0.00	0.00
Ni	0.96	0.94	1.07	1.17	0.95	0.00	0.00	0.16	0.15	0.17	0.13	0.10	0.11
Co	0.00	0.01	0.07	0.00	0.04	0.10	0.07	0.07	0.04	0.02	0.05	0.04	0.07
S	38.91	38.20	38.37	38.59	38.15	52.85	52.44	52.99	53.19	53.51	53.39	53.37	53.35
Total	99.24	99.21	99.32	99.90	99.35	100.21	100.18	100.04	100.10	100.38	100.00	100.00	99.81
V *apfu*	0.025	0.010	0.022	0.032	0.008	0.001	0.000	0.000	0.000	0.000	0.000	0.000	0.000
Cr	0.000	0.001	0.002	0.000	0.000	0.000	0.000	0.000	0.000	0.000	0.000	0.000	0.000
Fe	0.903	0.931	0.912	0.905	0.935	1.016	1.027	1.007	1.003	0.999	0.996	0.999	0.996
As	0.000	0.001	0.001	0.001	0.001	0.000	0.001	0.001	0.001	0.000	0.002	0.000	0.000
Ni	0.014	0.014	0.016	0.017	0.014	0.000	0.000	0.003	0.003	0.003	0.003	0.002	0.002
Co	0.000	0.000	0.001	0.000	0.001	0.002	0.001	0.001	0.001	0.000	0.001	0.001	0.001
S	1.057	1.043	1.046	1.045	1.041	1.981	1.971	1.987	1.992	1.996	1.999	1.998	2.000
Total	2.000	2.000	2.000	2.000	2.000	3.000	3.000	3.000	3.000	3.000	3.000	3.000	3.000

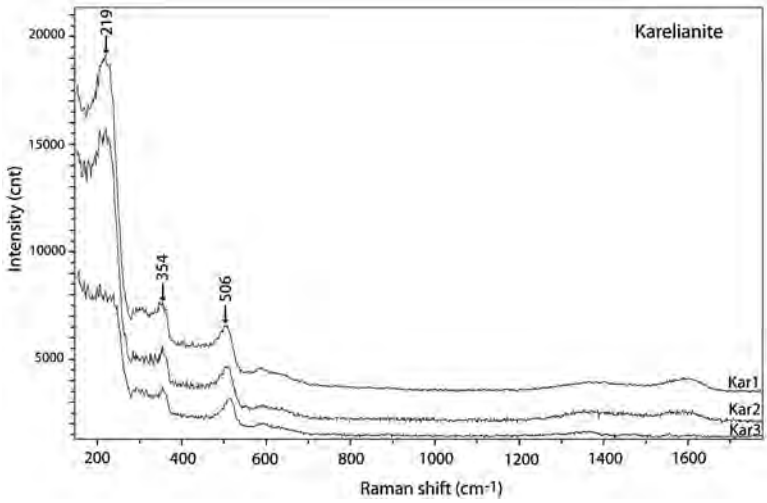

FIG. 5. Raman spectra of three grains of karelianite from Merelani Hills. The mineral is identified by its Raman lines at 219, 354 and 506 cm^{-1}.

Retrograde phases

A retrograde stage affected the karelianite–pyrrhotite assemblage (Fig. 1E). This episode seems contemporaneous with the formation of the "tanzanite"–pyrite II microveinlets. Mixtures of micrometric phases produced by destabilization of both karelianite and pyrrhotite are formed during the retrograde stage (Fig. 1F). The mixture at the boundary of karelianite grains is V-rich (up to 42 wt%), and the mixture developed near pyrrhotite is Fe-rich (up to 68 wt%).

DISCUSSION

Vanadium silicates or oxides are found in different types of deposits and in contrasting geological envi-

ronments. A spatial relationship between vanadium minerals and gold is described in gold telluride epithermal deposits (Lindgren 1907, Ahmad *et al*. 1987, Jensen & Barton 2000, Spry & Scherbarth 2006) and in mesothermal gold deposits (Gatehouse *et al*. 1983, Harris 1989, Pan & Fleet 1991, 1992). Roscoelite and vanadium-rich muscovite as well as the karelianite–eskolaite series are minerals spatially related with gold (Spry & Scherbarth 2006). Vanadium silicates and oxides and Cr–V spinels are reported in massive sulfide deposits (Long *et al*. 1963, Zakrzewski *et al*. 1982, Höller & Stumpfl 1995, Höller & Ghandi 1997, Canet *et al*. 2003), and geochemical anomalies in V and Cr are commonly used in exploration (Canet *et al*. 2004). The V–Cr–Ti oxides are also identified in metasedimentary sequences, such as in the Olkhon series from Lake Baikal (Koneva 2002, Döbelin *et al*. 2006), in the Chinese Shanglin and Hechi bitumens

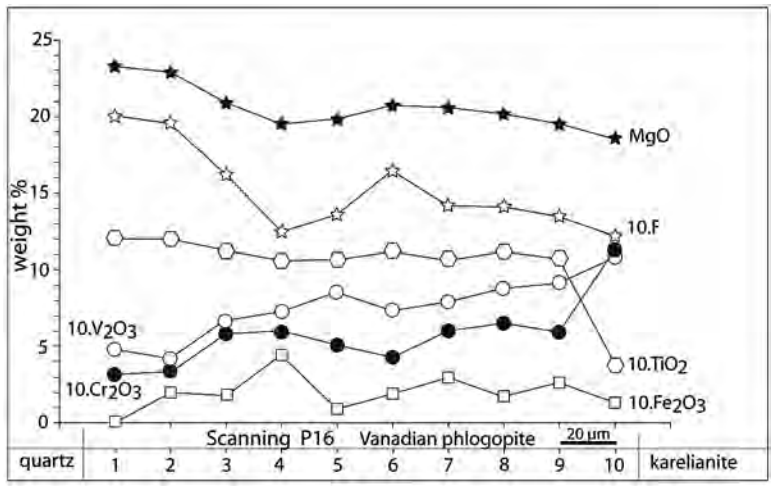

FIG. 6. EPMA scan across the zoned vanadian phlogopite in Figure 3 showing the distribution of various elements in the different zones detected in the X-ray images (cross section P16).

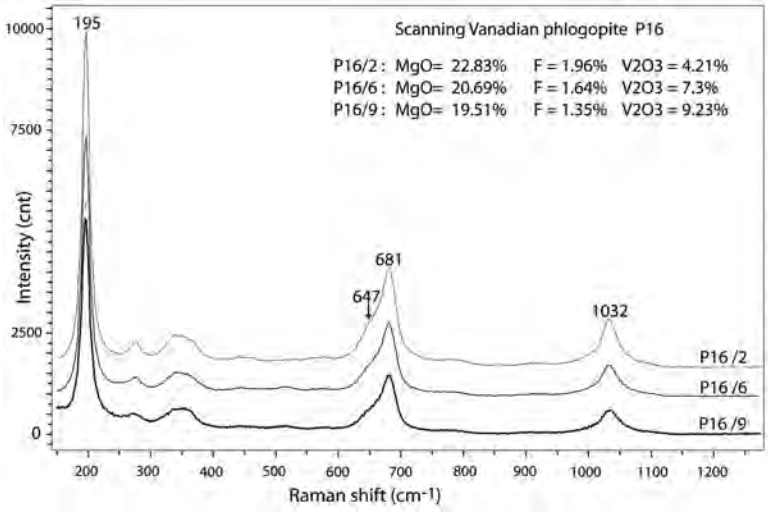

FIG. 7. Raman spectra of three grains of vanadian phlogopite of different chemical composition. The mineral is identified by its Raman lines at 195, 681 and 1032 cm^{-1}.

in Guangxi (Liu & Lin 1984) or in the Francevillian black shales and sandstones from the Mounana uranium deposit in Gabon (Geffroy *et al.* 1964, Gauthier-Lafaye & Weber 2003). Authigenic V oxides are found in Recent metalliferous sediments of the Red Sea (Jedwab *et al.* 1989).

A rare vanadian phlogopite is described in the Hemlo gold deposit in Ontario (Harris 1989, Pan & Fleet 1992), occurring as small flakes in micaceous or pyritiferous layers, in association with roscoelite. It is characterized by significant amounts of V (up to 10.1 wt% V_2O_3, which represents 0.58 V^{3+} *apfu*), TiO_2 (up to 1.07 wt%) and F (up to 0.5 wt%). The Mg/(Fe + Mg) value varies between 0.77 and 0.79. The vanadian phlogopite in the Merelani Hills tanzanite deposits is closely associated with karelianite in the graphite-bearing quartz veins. For comparison, V_2O_3 content is up to 10.9 wt% (0.63 V^{3+} *apfu*), TiO_2 up to 1.29 wt% and F up to 2 wt%. The Mg/(Fe + Mg) value is near 0.98. Compared to the solid solution formed in the Rampura Agucha (Höller & Stumpl 1995) and Lake Baikal suites of V–Cr oxides (Koneva 2002), the V–Cr oxides from the Tuvatu gold–silver prospect in Fiji (Spry & Scherbarth 2006) and the oxide from the "tanzanite" deposits from Merelani Hills are nearly pure karelianite (Fig. 4) with from 98.6 to 99.9, and from 93 to 96 wt% of V_2O_3, respectively. The Fe_2O_3 contents are very low for both occurrences 0.06 ± 0.03 and 0.33 ± 0.09 wt%, respectively, when compared to the 4.1 ± 0.5 wt% found in the Outokumpu karelianite (Long *et al.* 1963).

In most silicate minerals, vanadium is present as V^{3+}, which has an ionic radius similar to Al^{3+} in octahedral coordination (Shannon 1976, Fleet 2003). The substitution mechanism $Al^{3+} = V^{3+}$ is not clear in vanadian phlogopite, and therefore the amount of V is not directly controlled by the stoichiometric Al content at the octahedral site. Pan & Fleet (1992) discussed mechanisms of substitution in vanadian phlogopite at Hemlo. Their findings can also be applied to the vanadian phlogopite at Merelani Hills: i) $3Mg^{2+} = 2\ V^{3+}$ + a high proportion of vacancies at the octahedral sites (Table 2), ii) the substitution $Mg^{2+} + Si^{4+} = {}^{VI}V^{3+} + {}^{IV}Al^{3+}$, as suggested by the Si content in the vanadian phlogopite, which is less than 6 *apfu* (Fig. 8).

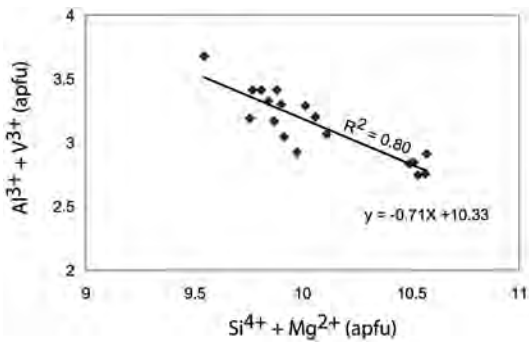

FIG. 8. $(Si^{4+} + Mg^{2+})$ *versus* $(Al^{3+} + V^{3+})$ diagram showing the mechanism of substitution in vanadian phlogopite.

In the Merelani Hills, karelianite is found in hydrothermal graphite-bearing quartz veins contained in a metasedimentary series of interbedded graphitic gneisses and marbles metamorphosed to the amphibolite facies. Originally, the host rock was a black shale, and the isotopic composition of carbon in graphite in the quartz veins ($\delta^{13}C = -24.0 \pm 1.0‰$) indicates a sedimentary precursor rich in organic matter. The vanadium and chromium contents of the graphitic gneisses are 446 and 72 ppm, respectively (Key & Ochieng 1991). In black shales, Cr and V are linked to the organic matter (Vine & Tourtelot 1970, Giuliani *et al.* 2000), and V may be concentrated in clays (Ripley *et al.* 1990) and chlorite (Wanty *et al.* 1990). Vanadium enrichment and the presence of organic matter indicate a sedimentary euxinic environment under reduced conditions (Brey & Wanty 1991). These V–Cr precursor minerals (clays ?) were consumed during prograde metamorphism to form graphite, sulfides and other Ca-silicate minerals in the graphitic gneisses and calc-silicates (vanadium-rich grossular).

During retrograde metamorphism, V and Cr were apparently scavenged by hydrothermal fluids from the graphitic gneisses and calc-silicates, at a temperature between 350 and 400°C (Malisa 1998). The H_2O-rich hydrothermal circulation led to the deposition of "tanzanite". Karelianite also formed during this hydrothermal stage, but was deposited early, at the contact with vanadium-bearing pyrrhotite as a discontinuous rim or as an infilling phase in dissolved regions of sulfide. The vanadian phlogopite crystallized after karelianite but is intimately associated with it. Both vanadian phases were later cross-cut by the graphite – "tanzanite" – quartz veinlets. The presence of karelianite implies vanadium enrichment in the fluid and consequently the presence of predominantly oxidizing conditions, as vanadium is more soluble in such redox conditions (Wehrli & Stumm 1989). Consequently, vanadium was fixed by karelianite and vanadian phlogopite upon reduction of the fluid at this stage, which was also enriched in magnesium and fluorine.

These vanadium minerals were affected at the hydrothermal stage, which corresponds to the formation of graphite – "tanzanite" – quartz veins. At this stage, textural evidence of dissolution of karelianite indicates that vanadium was probably remobilized by the hydrothermal fluid and fixed by "tanzanite". The chemical composition of the retrograde phases deposited at the contact between karelianite and pyrrhotite indicates that the metasomatic fluid mobilized not only vanadium from karelianite, but also iron and sulfur from the sulfide, and carried Si, Al and Ca, elements necessary for the formation of the vanadian zoisite ("tanzanite").

Conclusions

Karelianite and vanadian phlogopite were identified in graphite–"tanzanite"-bearing quartz veinlets hosted in graphitic gneisses of the Merelani Hills. Pure karelianite is intimately associated with vanadian phlogopite. The mineral composition and textural data suggest that V, Cr and C were mobilized throughout the whole metamorphic and hydrothermal stages. These elements were leached from the black shale protolith, and most likely Cr and V were associated with carbonaceous matter and clay minerals in the precursor euxinic sediments. These elements were mobilized during prograde metamorphism and concentrated during the retrograde hydrothermal episode to form V–(Cr) silicates and oxides such as vanadian grossular ("tsavorite"), vanadian zoisite ("tanzanite"), karelianite and vanadian phlogopite. Under oxidizing conditions, V and Cr became mobile hydrothermally, and the rare karelianite and vanadian phlogopite formed a source of vanadium for the formation of the gem-quality silicates.

Acknowledgements

We thank A. Kohler for the images obtained on the SEM Hitachi from the Université de Nancy I, and S. Mathieu and Y. Ravaux for their help with the electron microprobe at the Université de Nancy I. We are grateful to F. Mangasini of the University of Dar es Salaam for providing specimens. This research was supported by grants from the CRPG–CNRS and the IRD through the project "Géologie des gisements de corindon de Madagascar". We thank Dr. P. Burnard (CRPG–CNRS) for correcting the English of the earliest version of this paper. Dr. J.-C. Melgarejo (Universitat de Barcelona), Dr. C. Canet (Universidad Nacional Autonoma de Mexico), and an anonymous reviewer provided constructive reviews. The manuscript was also greatly improved by the comments and suggestions by the editor, Robert F. Martin.

References

Ahmad, M., Solomon, M. & Walshe, J.L. (1987): Mineralogical and geochemical studies of the Emperor gold telluride deposit, Fiji. *Econ. Geol.* **83**, 345-370.

Breit, G.N. & Wanty, R.B. (1991): Vanadium accumulation in carbonaceous rocks: a review of geochemical controls during deposition and diagenesis. *Chem. Geol.* **91**, 83-97.

Bridges, C.R. (1982): Gemstones of East Africa. *In* Proc. Gemological Symp. 1982 (D.M. Eash, ed.). Gemological Institute of America, Santa Monica, California (263-275).

Canet, C., Alfonso, P., Melgarejo, J.C. & Belyatski, B.V. (2004): Geochemical evidences of sedimentary-exhalative origin of the shale-hosted PGE–Ag–Au–Zn–Cu occurrences of the Prades Mountains (Catalonia, Spain): trace-element abundances and Sm–Nd isotopes. *J. Geochem. Explor.* **82**, 17-33.

Canet, C., Alfonso, P., Melgarejo, J.C. & Jorge, S. (2003): V-rich minerals in contact-metamorphosed Silurian sedex deposits in the Poblet area, southwestern Catalonia, Spain. *Can. Mineral.* **41**, 561-579.

Döbelin, N., Reznitsky, L.Z., Sklyarov, V., Armbruster, T. & Medenbach, O. (2006): Schreyerite $V_2Ti_3O_9$: a new occurrence and crystal structure. *Am. Mineral.* **91**, 196-202.

Fleet, M.E. (2003): *Rock-Forming Minerals*. **3A**. *Micas* (2nd ed.). The Geological Society, Bath, U.K.

Gatehouse, B.M., Grey, I.E. & Nickel, E.H. (1983): The crystal chemistry of nolanite $(V,Fe,Ti,Al)_{10}O_{14}(OH)_2$, from Kalgoorlie, Western Australia. *Am. Mineral.* **68**, 833-839.

Gauthier-Lafaye, G. & Weber, F. (2003): Natural nuclear fission reactors: time constraints for occurrence, and their relation to uranium and manganese deposits and to the evolution of the atmosphere. *Precamb. Res.* **120**, 81-100.

Geffroy, J., Cesbron, F. & Lafforgue, P. (1964): Données préliminaires sur les constituants profonds des minerais uranifères et vanadifères de Mounana (Gabon). *C.R. Acad. Sci. Paris* **259**, 601-603.

Giuliani, G., France-Lanord, C., Cheilletz, A., Coget, P., Branquet, Y. & Laumonier, B. (2000): Sulfate reduction by organic matter in Colombian emerald deposits: chemical and stable isotope (C, O, H) evidence. *Econ. Geol.* **95**, 1129-1153.

Harris, D.C. (1989): The mineralogy and geochemistry of the Hemlo gold deposit. *Geol. Surv. Can., Econ. Geol. Rep.* **38**.

Höller, W. & Ghandi, S.M. (1997): Origin of tourmaline and oxide minerals from the metamorphosed Rampura Agucha Zn–Pb–(Ag) deposit, Rajasthan, India. *Mineral. Petrol.* **60**, 99-119.

Höller, W. & Stumpfl, E.F. (1995): Cr–V oxides from the Rampura Agucha Pb–Zn–Ag deposit, Rajasthan, India. *Can. Mineral.* **33**, 742-745.

Hurlbut, C.S., Jr. (1969): Gem zoisite from Tanzania. *Am. Mineral.* **54**, 702-709.

Jedwab, J., Blanc, G. & Boulègue, J. (1989): Vanadiferous sediments from the Nereus Deep, Red Sea. *Terra Nova* **1**, 188-194.

Jensen, E.P. & Barton, M.D. (2000): Gold deposits related to alkaline magmatism. *Rev. Econ. Geol.* **13**, 279-314.

Key, R.M. & Ochieng, J.O. (1991): Ruby and garnet gemstone deposits in southeast Kenya: their genesis and recommendations for exploration. *In* African Mining '91 (Harare). Elsevier Science Publishers, Barking, Essex, U.K. (121-127).

KONEVA, A.A. (2002): Cr–V oxides in metamorphic rocks, Lake Baikal, Russia. *Neues Jahrb. Mineral., Monatsh.*, 541-550.

LINDGREN, W.T. (1907): Some gold and tungsten deposits of Boulder County, Colorado. *Econ. Geol.* **2**, 435-463.

LIU DEHAN & LIN MAOFU (1984): Discovery of some vanadium and nickel minerals from anthraxolite and discussion of their origin. *Scientia Sinica*, *Ser.* B, **27**, 1197-1202.

LONG, J.V.P., VUORELAINEN, Y. & KOUVO, O. (1963): Karelianite, a new vanadium mineral. *Am. Mineral.* **48**, 33-41.

MALISA, E. (1987): *Geology of the Tanzanite Gemstone Deposits in the Lelatema Area, NE Tanzania*. Ph.D. thesis, Annales Academicae Scintarium Fennicae III, Geologica-Geographica, Finland.

MALISA, E. (1998): Application of graphite geothermometer in hydrothermally altered metamorphic rocks of the Merelani–Lelatema area, Mozambique belt, northeastern Tanzania. *J. Afr. Earth Sci.* **26**, 313-316.

MALISA, E. & MUHONGO, S. (1990): Tectonic setting of gemstone mineralization in the Proterozoic metamorphic terrane of the Mozambique belt in Tanzania. *Precamb. Res.* **46**, 167-176.

MUHONGO, S., KRÖNER, A. & NEMCHIN, A.A. (2001): Single zircon evaporation and SHRIMP ages for granulite-facies rocks in Mozambique belt of Tanzania. *J. Geol.* **109**, 171-189.

MUHONGO, S., TUISKU, P. & MTONI, Y. (1999): Pan-African pressure–temperature evolution of the Merelani area in the Mozambique belt in northeast Tanzania. *J. Afr. Earth Sci.* **29**, 353-365.

NAESER, C.W. & SAUL, J. M. (1974): Fission track dating of tanzanite. *Am. Mineral.* **59**, 613-614.

ORLANDI, P., PASERO, M., DUCHI, G. & OLMI, F. (1997): Dessauite, (Sr,Pb) (Y,U) (Ti, Fe^{3+})$_{20}O_{38}$, a new mineral of the crichtonite group from Buca della Vena mine, Tuscany, Italy. *Am. Mineral.* **82**, 807-811.

PAN, YUANMING & FLEET, M.E. (1991): Vanadian allanite-(La) and vanadian allanite-(Ce) from the Hemlo gold deposit, Ontario, Canada. *Mineral. Mag.* **79**, 497-507.

PAN, YUANMING & FLEET, M.E. (1992): Mineral chemistry and geochemistry of vanadian silicates in the Hemlo gold deposit, Ontario, Canada. *Contrib. Mineral. Petrol.* **109**, 511-525.

POUCHOU, J.L. & PICHOIR, F. (1991): Quantitative analysis of homogeneous or stratified microvolumes applying "PAP". *In* Electron Probe Quantitation (K.F.J. Heinrich & D.E. Newbury, eds.). Plenum Press, New York, N.Y. (31-75).

RIPLEY, E.M., SHAFFER, N.R. & GILSTRAP, M.S. (1990): Distribution and geochemical characteristics of metal enrichment in the New Albany shale (Devonian–Mississippian), Indiana. *Econ. Geol.* **85**, 1790-1807.

SHANNON, R.D. (1976): Revised effective ionic radii and systematic studies of interatomic distances in halides and chalcogenides. *Acta Crystallogr.* **A32**, 751-757.

SPRY, P.G. & SCHERBARTH, N.L. (2006): The gold–vanadium–tellurium association at the Tuvatu gold–silver prospect, Fiji: conditions of ore deposition. *Mineral. Petrol.* **87**, 171-186.

TRELOAR, P.J. (1987): The Cr-minerals of Outokumpu – their chemistry and significance. *J. Petrol.* **28**, 867-886.

VINE, J.D. & TOURTELOT, E.B. (1970): Geochemistry of black shale deposits – a summary report. *Econ. Geol.* **65**, 253-272.

VON KNORRING, O., CONDLIFFE, E. & TONG, Y.L. (1986): Some mineralogical and geochemical aspects of chromium-bearing skarn from northern Karelia, Finland. *Geol. Soc. Finland Bull.* **58**, 277-292.

WALTON, L. & MARSHALL, D. (2007): Tanzanite and tsavorite. *Mineral. Assoc. Can., Short Course* **37**, 153-160.

WANTY, R.B., GOLDHABER, M.B. & NORTHROP, H.R. (1990): Geochemistry of vanadium in an epigenetic, sandstone-hosted vanadium–uranium deposit, Henry Basin, Utah. *Econ. Geol.* **85**, 270-284.

WEHRLI, B. & STUMM, W. (1989): Vanadyl in natural waters; adsorption and hydrolysis promote oxygenation. *Geochim. Cosmochim. Acta* **53**, 69-77.

ZAKRZEWSKI, M.A., BURKE, E.A.J. & LUSTENHOUWER, W.J. (1982): Vuorelainenite, a new spinel, and associated minerals from the Sätra (Doverstorp) pyrite deposit, central Sweden. *Can. Mineral.* **20**, 281-290.

ZANCANELLA, V. (2006): La tanzanite. *Revue de gemmologie* **156**, 6-10.

Received December 23, 2007, revised manuscript accepted August 23, 2008.